Collisions of electrons with interstellar grains

D. R. Flower ⬤★

Physics Department, University of Durham, Durham DH1 3LE, UK

ABSTRACT

We have computed cross-sections for elastic and inelastic scattering of electrons on small grains at low-collision energies. Significant differences are again found between the results obtained in the presence and the absence of a 'permanent' grain dipole moment. In addition to spherical grains, scattering on ellipsoidal grains is investigated. We conclude that the rate of electron attachment to interstellar grains may be substantially lower in regions of molecular clouds from which the radiation field is excluded, and where the grains are less likely to possess a dipole moment.

Key words: astrochemistry – molecular processes – scattering – ISM: molecules.

1 INTRODUCTION

A knowledge of the rate of electron capture by grains, particularly small grains, is essential for determining the charge state of interstellar molecular clouds (Draine & Sutin 1987), which are also the regions of star formation. At the low temperatures ($T \lesssim 100\,\mathrm{K}$), and hence low electron collision energies, which prevail in such clouds, the techniques of quantum mechanics are, a priori, more appropriate to studying electron–grain scattering than are classical mechanics.

In a recent paper (Flower 2022), we used the methods of quantum mechanics to calculate the electron–grain momentum-transfer cross-section, extending earlier work by Flower & Middleton (2004) by considering attachment not only to neutral but also to charged grains, and to grains possessing a permanent dipole moment (Jordan & Weingartner 2009). It was found that the presence of a dipole moment had significant consequences for electron–grain scattering, as expressed through the momentum-transfer (diffusion) cross-section

$$\sigma_\mathrm{d} = 2\pi \int_0^\pi I(\Theta)(1 - \cos\Theta)\sin\Theta\,\mathrm{d}\Theta \tag{1}$$

particularly in the case of grains with no net charge ($Q = 0$). In equation (1), $I(\Theta)$ is the differential cross-section for scattering through angle Θ, and σ_d is the diffusion cross-section. Specifically, the presence of a permanent dipole moment reduced the discrepancies, at low-collision energies E, between the diffusion cross-section and the classical cross-section, as derived on the assumption that the electron orbits the grain when the centrifugal repulsion is balanced by the attractive image potential (Draine & Sutin 1987)

$$V(r) = -\frac{\epsilon - 1}{\epsilon + 2}\frac{q^2\alpha}{2r^2(r^2 - a^2)}, \tag{2}$$

where ϵ is the dielectric constant of the grain and $q = -e$ is the electron charge; r is the distance of the electron from the centre of the grain. supposed spherical and of radius a; $\alpha = a^3$ is the polarizability of the grain.

★ E-mail: david.flower@durham.ac.uk

The image potential, equation (2), is singular at $r = a$, where it presents an infinite potential wall to the electron. For this reason, quantum mechanical calculations that use the image potential predict that the diffusion cross-section tends to the geometrical cross-section, πa^2, as E increases; but the singularity in the potential is unphysical, casting doubt on the results obtained at high-collision energies. Furthermore, the extent to which the cross-section at low energies might be modified by the use of a more realistic short-range potential needs to be established; this was one of the aims of the present study.

The shapes of interstellar grains are not known; but the assumption that they are spherical is unlikely to be correct. Accordingly, we investigated the interaction of electrons with the simplest form of non-spherical grains – ellipsoids – which have two, perpendicular symmetry axes with differing polarizabilities.

In the following Section 2, we describe the grain models that we have used and illustrate the influence of both a more realistic electron–grain interaction potential and the non-sphericity of the grains. Our conclusions are summarized in Section 3.

2 A QUANTUM MECHANICAL MODEL OF ELASTIC AND INELASTIC ELECTRON–GRAIN COLLISIONS

2.1 Interaction potential

In our previous studies of electron–grain collisions, the polarization (charge-induced-dipole) potential was assumed to take the form of the image potential, equation (2), which derives from classical image-charge theory (cf. Jackson 1962). The image potential is singular and changes sign at $r = a$, and the momentum-transfer cross-section tends to the geometrical cross-section of the grain at high-collision energies. This limit is reached as the de Broglie wavelength

$$\lambda = 2\pi\left(\frac{2mE}{\hbar^2}\right)^{-\frac{1}{2}}$$

© 2024 The Author(s).

becomes smaller that the dimension of the grain. In this expression, m is the mass and E the kinetic energy of the electron.

Given that the presence of a singularity in V is non-physical, it is pertinent to consider other forms of the potential that are more realistic at short range. A simple, but more physically correct, approximation of the interaction potential[1] would comprise equation (2) for $r > a + d$, where d is the solution of

$$\frac{\epsilon - 1}{\epsilon + 2} \frac{q^2 a^3}{2(a+d)^2(d^2 + 2ad)} = W + E_F, \tag{3}$$

and

$$V(r) = -(W + E_F) \tag{4}$$

for $r < a + d$. In equations (3) and (4), W is the work function and E_F is the *Fermi* energy of the grain. Thus, the potential wall at $r = a$ is replaced by a potential well of depth $W + E_F$ for $r < a + d$, thereby enabling the electron to penetrate the grain interior. In practice, we varied the value of d in order to investigate the dependence of the cross-section on the value of the well depth. We note that, when $d < < a$, the well depth is given approximately by

$$W + E_F = \frac{\epsilon - 1}{\epsilon + 2} \frac{q^2}{4d}$$

and is independent of a.

2.2 Diffusion cross-section

2.2.1 Dipole moment p = 0

In order to illustrate the consequences of replacing the potential wall of equation (2) by the potential well of equation (4), we consider first a case in which the dipole moment of the grain, $p = 0$. We adopt $a = 0.001 \, \mu$m (10 Å) for the dimension of the grain and either $a + d = 1.01a$ ($d = 0.1$ Å) or $a + d = 1.02a$ ($d = 0.2$ Å) for the radius of the potential well, corresponding to well depths of 14 eV and 7 eV, respectively; these values are comparable with the ionization potentials of cyclic aromatic hydrocarbons and fullerenes, as reported by Omont (1986) and Weingartner & Draine (2001). As in our previous study (Flower 2022), we take $\epsilon = 3$.

In Fig. 1 are plotted the momentum transfer cross-section, computed assuming a potential well, and the classical 'orbiting' cross-section, obtained assuming a potential wall. It may be seen that the results for the two values of d are similar and both deviate from the classical cross-section at both low- and high-collision energies. When $E/k_B > 10^5$ K, $E \gtrsim 10$ eV, which is comparable with the well depth. As E increases further, the incoming electron becomes progressively unaware of the presence of the scattering dust particle.

At low energies ($E/k_B < 10^2$ K, $E \lesssim 10$ meV), the cross-section

$$\sigma = \sum_{l=0}^{l_{max}} \sigma_l.$$

is dominated by a single-partial wave, $l = 1$; l is the angular momentum quantum number of the electron, relative to the grain. The 'effective' potential

$$V_{eff}(r) = V(r) + \frac{l(l+1)\hbar^2}{2mr^2}$$

is the sum of the (attractive) electrostatic potential, $V(r)$, and the (repulsive) centrifugal potential, which, for $l > 1$, prevents the
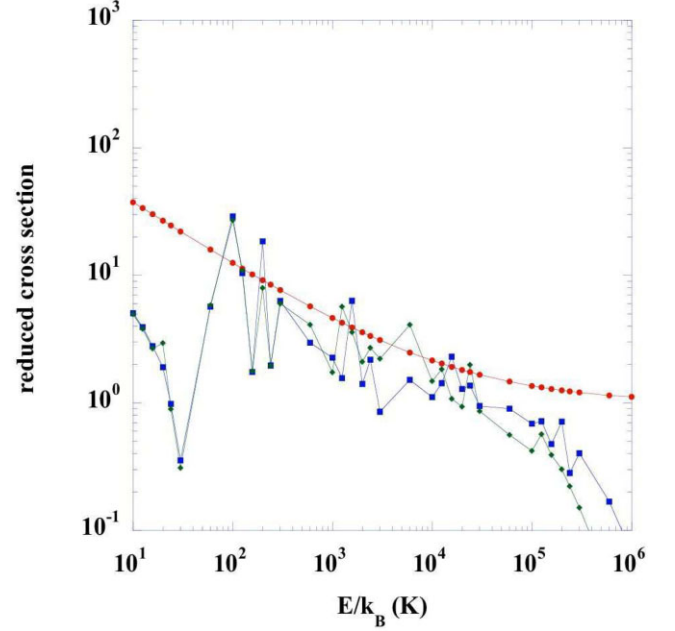
[1]This approximation was suggested to the author by the anonymous referee of Flower (2022).

Figure 1. The reduced momentum transfer (diffusion) cross-section, $\sigma/\pi a^2$, as a function of the collision energy, E/k_B (K). for $a = 0.001 \, \mu$m; the grain dipole moment $p = 0$. Results obtained with a potential well (equation 4) and $d/a = 0.01$ are shown as the blue curve, and with $d/a = 0.02$ as the green curve. The classical cross-section, derived from the orbiting approximation, is plotted also (red curve).

electron from attaining the potential well. Under these circumstances, the cross-section becomes independent of the value of d, and hence of the well depth, and is much smaller than predicted by the classical orbiting approximation. Indeed, orbiting in the classical sense is not possible for $E/k_B \lesssim 50$ K, as the energy of the electron is less than the height of the effective potential barrier. Subsequently, for $E/k_B \approx 50$ K, the cross-section increases, by more than an order of magnitude, owing to the progressive contribution of partial waves $l > 1$, and becomes consonant with the classical orbiting approximation, when averaged over the wave-mechanical interference effects.

2.2.2 Dipole moment p > 0

We now turn to the case in which the grain possesses an intrinsic dipole moment and the interaction potential is given by

$$V(r, \theta) = \frac{qp}{r^2} \cos \theta - \frac{\epsilon - 1}{\epsilon + 2} \frac{q^2 a^3}{2r^2(r^2 - a^2)}, \tag{5}$$

where θ is the angle between the grain dipole-moment vector, **p**, and the electron position vector, **r**. In practice, we adopt $p = ea$ (cf. Jordan & Weingartner 2009, who considered silicate grains explicitly), as in our previous work (Flower 2022). We use the same values of d, and hence of the well depths (14 eV and 7 eV), as in subsection 2.2.1. We note from fig. 5 of Weingartner & Draine (2001) that the ionization potentials of neutral silicate and graphite grains – approximately 8 eV and 7 eV, respectively – lie in this range of well depth. Furthermore, as will be seen in Fig. 2, the diffusion cross-section is insensitive to the value of the well depth at low-collision energies ($E/k_B \lesssim 1000$ K) and temperatures, which are the most relevant here.

We show first, in Fig. 2, the momentum transfer cross-section calculated for a grain size $a = 0.001 \, \mu$m (10 Å), and $d/a = 0.01$ and $d/a =$
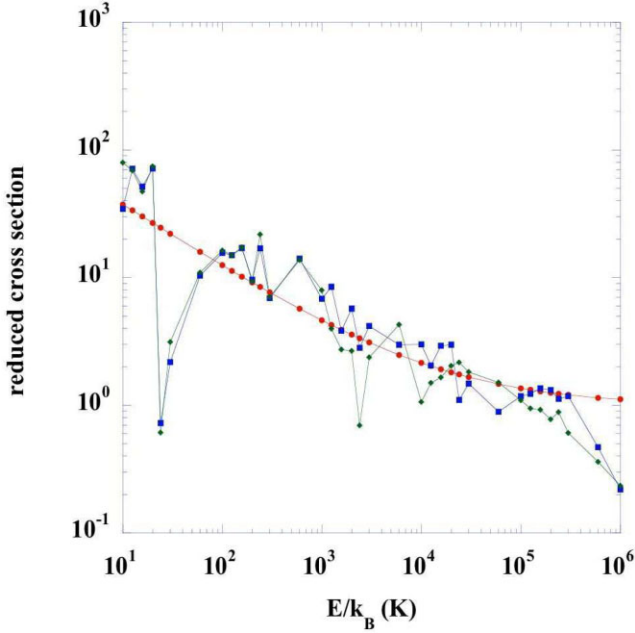
Figure 2. The reduced momentum transfer (diffusion) cross-section, $\sigma/\pi a^2$, as a function of the collision energy, E/k_B (K). for $a = 0.001\,\mu$m; the grain dipole moment $p = ea$. In equation (3), $d/a = 0.01$ (blue curve) and $d/a = 0.02$ (green curve); the classical cross-section, derived from the orbiting approximation, is shown also (red curve). Note that the polarizability, a^3, and dipole moment, ea, depend on a.

0.02, corresponding to well depths of 14 eV and 7 eV, respectively; Fig. 2 may be compared directly to Fig. 1, where $p = 0$. At high-collision energies, E, the systematic deviation from the classical cross-section, based on the orbiting approximation, is again apparent. At low energies ($E/k_B \lesssim 100$ K), the inclusion of the dipole potential, which has the same r^{-2}-dependence as the centrifugal potential, has a significant effect on the results. Although the dipole term contributes only through inelastic collisions, owing to its θ-dependence, the effective rotational constant

$$B = \frac{\hbar^2}{2I}$$

and the corresponding excitation energies are taken to be very small, compared with the collision energy, in view of the high moment of inertia, I, of the grains; and hence the scattering process is quasi-elastic.

Analogous results for a larger grain, $a = 0.01\,\mu$m (100 Å), are shown in Fig. 3; the values of d (and corresponding well depth) in this case are $d/a = 0.002$ (7 eV). It may be seen that the wave-mechanical and classical cross-sections deviate systematically only for collision energies $E/k_B > 10^5$ K ($E \gtrsim 10$ eV), that is, for collision energies greater than the well depth.

2.2.3 Validity of the orbiting approximation

When deriving the classical cross-section, it was assumed that there is an 'orbiting' radius at which the centrifugal repulsion, which is proportional to r^{-2}, is balanced exactly by the attractive image potential, which varies as r^{-4} at long range. To this orbiting radius, there corresponds a limiting value of the impact parameter, b, given by
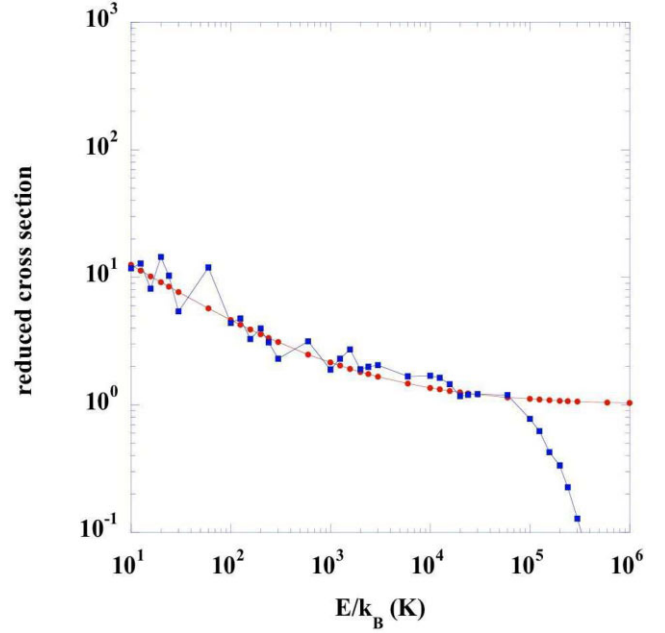

Figure 3. The reduced momentum transfer (diffusion) cross-section, $\sigma/\pi a^2$, as a function of the collision energy, E/k_B (K). for $a = 0.01\,\mu$m; the grain dipole moment $p = ea$. In equation (3), $d/a = 0.002$ (blue curve); the classical cross-section, derived from the orbiting approximation, is shown as the red curve.

$$\frac{b^2}{a^2} = 1 + 2\left(\frac{\epsilon - 1}{\epsilon + 2}\frac{e^2}{2aE}\right)^{\frac{1}{2}}, \tag{6}$$

where E is the collision energy; the classical cross-section is $\sigma = \pi b^2$. As $E \to \infty$, $b \to a$, owing to the presence of the infinite wall at $r = a$ in the image potential; but the introduction of a potential well for $r \le a + d$ invalidates this high-energy behaviour.

The relevance of the orbiting approximation depends on the assumption that the probability of a reaction – in the present case, of attachment – is enhanced, owing to the relatively long time that the incoming particle spends in proximity to the target. In the presence of a potential well, an alternative classical criterion could be the limiting value of b for which the point of closest approach of the incoming electron is equal to the radius, $a + d$, of the spherical potential well. At this point,

$$\frac{L^2}{2\mu(a+d)^2} = \frac{\epsilon - 1}{\epsilon + 2}\frac{q^2 a^3}{2(a+d)^2[(a+d)^2 - a^2]} + E, \tag{7}$$

where $L^2 = 2\mu E b^2$ is the square of the orbital angular momentum of the electron. Equation (7) takes the form

$$\frac{b^2}{a^2} = x^2\left(\frac{\epsilon - 1}{\epsilon + 2}\frac{q^2}{2aEx^2(x^2 - 1)} + 1\right), \tag{8}$$

where $x = 1 + d/a$. When the first term in brackets on the right hand side is much greater than 1, $\sigma \propto E^{-1}$. The corresponding quantum mechanical expression is obtained on setting $L^2 = l(l+1)\hbar^2$, whence

$$l(l+1)\hbar^2 = 2\mu a^2 x^2 E\left(\frac{\epsilon - 1}{\epsilon + 2}\frac{q^2}{2aEx^2(x^2 - 1)} + 1\right). \tag{9}$$

If the first term in brackets on the right hand side is much greater than 1,

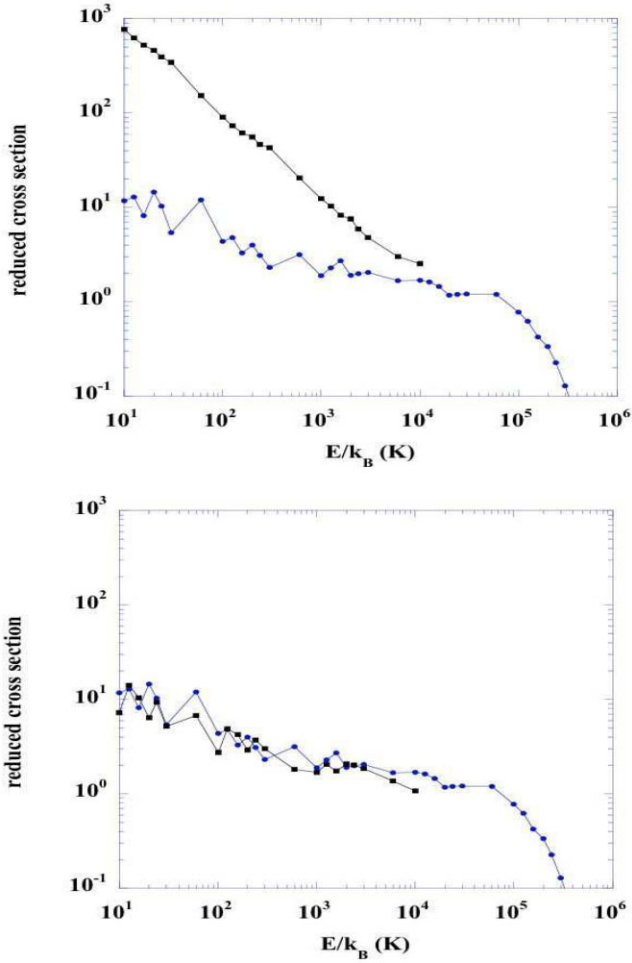$$l(l+1) \approx \frac{\epsilon - 1}{\epsilon + 2}\frac{a}{a_0(x^2 - 1)}, \tag{10}$$

Figure 4. The reduced momentum transfer (diffusion) cross-section, $\sigma/\pi a^2$, as a function of the collision energy, E/k_B (K), for $a = 0.01\ \mu$m; the grain dipole moment $p = ea$ (upper panel) or $p = 0$ (lower panel). In equation (3), $d/a = 0.002$. The cross-section that derives from the orbiting approximation, is shown as the blue curve, and that which derives from equation (10) as the black curve; see text, subsection 2.2.3.

where $a_0 = 0.5292 \times 10^{-8}$ cm is the atomic unit of length (the Bohr radius). In practice, the nearest integral value of $l \equiv l_{max}$ is taken to be the upper limit in the sum of the partial cross-sections, σ_l, over l, which determines the total momentum-transfer cross-section

$$\sigma = \sum_{l=0}^{l_{max}} \sigma_l.$$

The corresponding values of the diffusion cross-section are shown, as functions of the collision energy, in Fig. 4, where they are compared with the results of the 'orbiting' model, for the parameters of Fig. 3. When these parameters are adopted, equation (10) is valid for $E/k_B \lesssim 10^4$ K.

It may be seen from the upper panel of Fig. 4 that, when $p = ea$, the cross-section that derives from the orbiting approximation (the blue curve) lies below that which derives from equations (10) (the black curve) for $E/k_B \lesssim 10^4$ K, with the difference approaching two orders of magnitude at $E/k_B = 10$ K. The trend line of the black curve for $E/k_B \lesssim 10^4$ K is approximately consistent with $\sigma \propto E^{-1}$, as anticipated. The reason for the difference in the models at low energies is that the orbiting criterion excludes the contribution to the cross-section from relative angular momenta (equivalently, impact
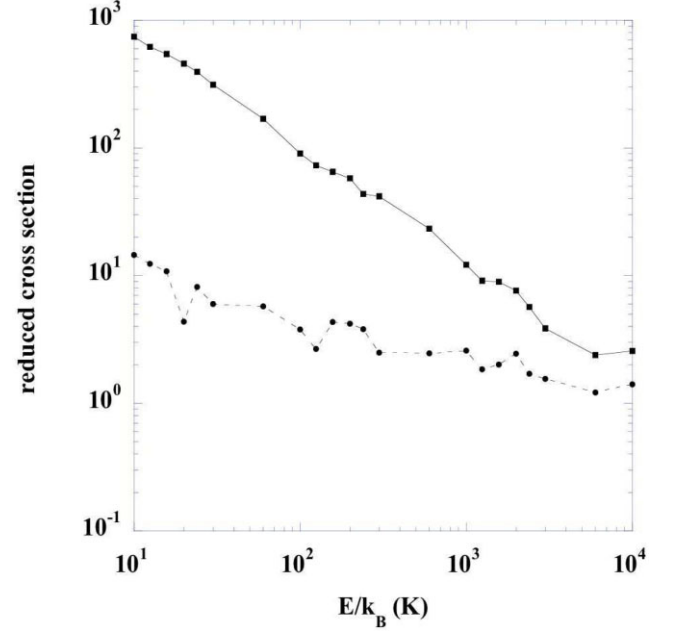

Figure 5. The reduced momentum transfer (diffusion) cross-section, $\sigma/\pi a^2$ of ellipsoidal grains, as a function of the collision energy, E/k_B (K), for $a = 0.01\ \mu$m, $d/a = 0.002$, and $p = ea$ (full curve) or $p = 0$ (broken curve). See text, subsection 2.2.4.

parameters) that are too large for orbiting to occur. We note that the enhancement of the diffusion cross-section that is seen in Fig. 4 is associated entirely with the presence of the grain dipole moment, $p = ea$. When $p = 0$, the cross-section that derives from equation (10) yields results (for $E/k_B \lesssim 10^4$ K) that do not differ significantly from from the orbiting approximation: see the lower panel of Fig. 4.

2.2.4 Ellipsoidal grains

The alignment of grains in a magnetic field has long been recognized as being responsible for the polarization of starlight (Hall 1949) and implies the presence of non-spherical grains. The simplest model that can be adopted is that the grains are ellipsoids, of effective radius (Draine & Hensley 2021)

$$a = (a_1 a_2 a_3)^{\frac{1}{3}},$$

where 1, 2, and 3 denote the principal axes. We assume the grains to be spheroids, elongated along one axis (prolate) and having optical and electrical properties that differ along this and any perpendicular axis. Thus, the mean polarizability of the grain

$$\alpha = \frac{\alpha_\parallel + 2\alpha_\perp}{3},$$

where $\alpha_\parallel$ and $\alpha_\perp$ are the polarizabilities parallel and perpendicular to its extension axis. In this case, there is an extra contribution to the interaction potential,

$$-\frac{\alpha_\parallel - \alpha_\perp}{3r^4} \frac{3\cos^2\theta - 1}{2},$$

which is θ-dependent, varies as r^{-4} and is proportional to $(\alpha_\parallel - \alpha_\perp)$; for the purpose of this illustration, we adopted $(\alpha_\parallel - \alpha_\perp)/\alpha = 0.3$, corresponding to an eccentricity of approximately 0.85 for prolate spheroidal grains (Krügel 2008).

Although this additional term in the potential contributes only through inelastic collisions, owing to its θ-dependence, the excitation

energies are very small, compared with the collision energy, and the process is quasi-elastic. Thus, the interaction potential may be considered to have acquired a quasi-elastic term that varies as r^{-4} for all values of r, including $r < a + d$. However, as may be seen by comparing the results in Fig. 5 with the corresponding curves in Fig. 4 (for $p = ea$ and $p = 0$), the additional term in the potential has only modest effects. Alternatively, we see once again the much greater influence of introducing a finite grain dipole moment, $p = ea$, whose presence enhances the cross-section, particularly at low temperatures.

3 CONCLUDING REMARKS

We have studied elastic and inelastic scattering of electrons on small grains, making various assumptions regarding the form of the interaction potential, relating to the presence of a finite dipole moment on, or the non-sphericity of, the grains. We find that the introduction of a grain-dipole-moment is sufficient in itself to lead to agreement of cross-sections derived from the classical 'orbiting' approximation and quantum mechanical calculations of the momentum-transfer ('diffusion') cross-section, even at the low energies ($E/k_B \lesssim 10^2$ K) that characterize interstellar molecular clouds. Alternatively, in the absence of a dipole moment, the diffusion cross-section at low energies falls below the prediction of classical mechanics.

Jordan & Weingartner (2009) considered that the hole that constitutes the positive charge of the grain dipole is created by photodetachment of an electron, whilst the electron that constitutes the negative charge is generated by electron collisional attachment. If this were the case, grains would be expected to possess a non-zero (time averaged) dipole moment in regions that are exposed to ultraviolet radiation, but not in the cold, molecular regions of interstellar clouds, which are shielded from the radiation field. There, the rate of electron attachment to the grains, including the small grains considered here, would be considerably lower, and the density of free electrons in the gas phase would be correspondingly higher

than anticipated on the basis of classical estimates of the rate of electron attachment to grains. The free electrons would recombine with positive ions, thereby reducing the degree of ionization of the medium. Dissociative recombination of electrons with molecular ions, such as H_3^+ and HCO^+, would inhibit the formation of heavier, more complex molecules in the gas-phase. Thus, a reduced rate of electron attachment to small grains could have important consequences for both the molecular composition and the dynamics of the cores of molecular clouds. Calculations of the grain charge using a rate of electron attachment that is much smaller, at low temperatures, than predicted by the classical model (cf. Figs 1 and 2 earlier) are required to test this hypothesis.

DATA AVAILABILITY

The data generated by this study are available on request to the author.

REFERENCES

Draine B. T., Hensley B. S., 2021, ApJ, 910, L47
Draine B. T., Sutin B., 1987, ApJ, 320, L803
Flower D. R., 2022, MNRAS, 517, 175
Flower D. R., Middleton M. J., 2004, MNRAS, 352, 837
Hall J. S., 1949, Science, 109, 166
Jackson J. D., 1962, Classical Electrodynamics. Wiley, New York
Jordan M. E., Weingartner J. C., 2009, MNRAS, 400, 536
Krügel E., 2008, An Introduction to the Physics of Interstellar Dust. Taylor & Francis, New York
Omont A., 1986, A&A, 164, 159
Weingartner J. C., Draine B. T., 2001, ApJS, 134, 263

This paper has been typeset from a TeX/LaTeX file prepared by the author.